JHEP02 (2016) 006

Triple Higgs boson production at a 100 TeV proton-proton collider

Andreas Papaefstathiou[a] **and Kazuki Sakurai**[b]

[a]*PH Department, TH Unit, CERN,*
CH-1211 Geneva 23, Switzerland

[b]*Department of Physics, Theoretical Particle Physics & Cosmology,*
King's College London, U.K.

E-mail: apapaefs@cern.ch, kazuki.sakurai@kcl.ac.uk

ABSTRACT: We consider triple Higgs boson production at a future 100 TeV proton-proton collider. We perform a survey of viable final states and compare and contrast triple production to Higgs boson pair production. Focussing on the $hhh \to (b\bar{b})(b\bar{b})(\gamma\gamma)$ final state, we construct a baseline analysis for the Standard Model scenario and simple deformations, demonstrating that the process merits investigation in the high-luminosity phase of the future collider as a new probe of the self-coupling sector of the Higgs boson.

Contents

1 Multi-Higgs boson production at hadron colliders

With the exception of very few interactions, most of the terms that comprise the Standard Model (SM) Lagrangian have been measured or constrained, their strengths found to be suggestively close to the expected ones. An important category of interactions *not* directly observed are those of the the Higgs boson with itself. The so-called 'self-couplings' and their energy dependence are crucial in determining the stability of the vacuum. Current observations suggest that our Universe may be sitting at a metastable false vacuum [1–8] and measurements of these couplings will illuminate this fact further.

At colliders, these terms, i.e. those proportional to h^n, h being the Higgs boson scalar field, can be directly probed through the simultaneous production of $(n-1)$ Higgs bosons. Unfortunately, the production rates for processes with $n \geq 3$, i.e. more than one Higgs boson, are small, mainly due to the relatively large invariant mass of the final state system. In particular, at the Large Hadron Collider (LHC) with 14 TeV proton-proton centre-of-mass energy, gluon-fusion Higgs boson pair production is expected to have a cross section of ∼40 fb [9–17], whereas triple production is expected to have a rather dwarfish rate, with a cross section of $\mathcal{O}(0.1$ fb) [15]. Hence, even though there is optimism that Higgs boson pair production will provide important information and constraints through LHC measurements [18–75], any direct measurement of SM-like triple Higgs boson production will be essentially impossible at the LHC, even at the end of the high-luminosity phase (HL-LHC) [76, 77]. However, with a significant increase in the collision energy, a Future

Circular hadron-hadron Collider (FCC-hh), colliding protons at 100 TeV, stands a good chance at observing and constraining the self-coupling of the Higgs bosons through Higgs boson pair production [64, 71, 78–80], the cross section rising to ~ 1.6 pb [81]. Additionally, at the FCC-hh one may also get the chance to observe three on-shell Higgs bosons being produced, since the total cross section rises to ~ 5 fb [15]. The evaluation of this possibility is the main object of the present article.

Concretely, the part of the Higgs boson potential which includes the self-interactions, may be written as:

$$\mathcal{V}_{\text{self}} = \frac{m_h^2}{2v} \left(1 + c_3\right) h^3 + \frac{m_h^2}{8v^2} \left(1 + d_4\right) h^4 \,, \tag{1.1}$$

where $v \simeq 246$ GeV is the vacuum expectation value (vev), $m_h \simeq 125$ GeV is the measured Higgs boson mass and c_3 and d_4 parametrize possible deviations from the standard model expectation (i.e. the SM is recovered for $c_3 = d_4 = 0$).

Figure 1 shows some of the Feynman diagrams contributing to triple Higgs boson production. It is clear that the production cross section depends on both c_3 and d_4 parameters. This should be contrasted to double Higgs boson production, which does not depend on d_4. In ref. [76] the dependence of the triple Higgs boson cross section on the parameters c_3 and d_4 was investigated at 14 TeV and 200 TeV proton-proton colliders for a Higgs boson mass $m_h = 120$ GeV. We produce an equivalent result for proton-proton collisions at 100 TeV, for $m_h = 125$ GeV, shown in figure 2. The conclusions are similar to those drawn in [76]: the cross section dependence on d_4 is mild, the deviations due to $d_4 = \pm 1$ being at most $\pm 20\%$ for $c_3 = 1$. Hence modifications of the d_4 coefficient itself will be very challenging to probe. This is also demonstrated in the contour plot of figure 3(a), which shows the cross section normalised to the SM value, on the $c_3 - d_4$ parameter space. On this plane, one can observe that the dependence along d_4 is much weaker than that along c_3.

In terms of constraining c_3, triple Higgs boson production cannot be superior to double Higgs boson production due to its small production cross section. On the other hand, triple production would be the best process to constrain d_4, although, as we will demonstrate, even the FCC-hh with 30 ab^{-1} of integrated luminosity can only provide $\mathcal{O}(1)$ constraints on d_4, because its dependency of the cross section is very modest. However, observing the triple Higgs boson production process is an interesting task in its own right, and as will be seen, indeed challenging at the FCC-hh. The goal of this article is to provide a first baseline study of Standard Model-like triple Higgs boson production via gluon fusion (ggF), at a future 100 TeV proton-proton collider. Furthermore, we investigate triple Higgs production in two scenarios where it is affected by new physics: (i) in the SM augmented by a single higher-dimensional operator in an effective field theory approach and (ii) the generic case on the $(c_3 - d_4)$-plane.

The article is organised as follows: in section 1.1 we investigate an explicit scenario that contains a single higher-dimensional operator. In section 2 we list, for future reference, the final states that could be interesting in the study of Higgs boson triple production. The Monte Carlo event generation, simulation of b-jet and photon tagging are described in section 3. Differential distributions at parton level for triple Higgs boson production at 100 TeV, compared to those of Higgs boson pair production and the analysis of the channel
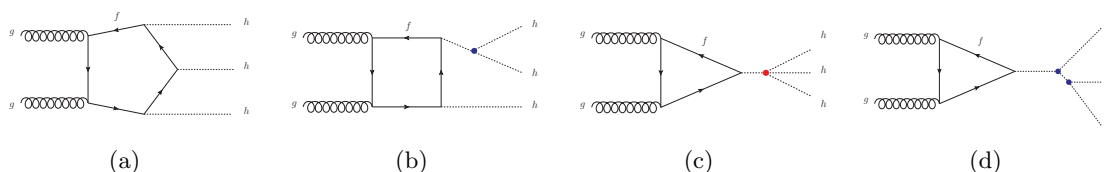
Figure 1. Example Feynman diagrams contributing to Higgs boson triple production via gluon fusion in the Standard Model. The vertices highlighted with a blobs indicate either triple (blue) or quartic (red) self-coupling contributions.

$(b\bar{b})(b\bar{b})(\gamma\gamma)$ is described in section 4. We use this analysis to provide constraints in two scenarios. Finally, we provide discussion and conclusions in section 5.

1.1 The self-coupling in $D = 6$ EFT

In the framework of the dimension-6 operator extension to the Standard Model ($D = 6$ EFT), one can compare the sensitivity of multi-Higgs production to variations of the operator Wilson coefficients [50]. Here we consider, as an illustrative example, a simplified mode with the assumption that the effect of all coefficients apart from a single one, originating from an operator of the form $\mathcal{O}_6 \sim |H|^6$, where H is the Higgs doublet scalar before electroweak symmetry breaking:

$$V_{\text{self}} = \mu^2|H|^2 + \lambda|H|^4 + \mathcal{O}_6, \ \mathcal{O}_6 \equiv \frac{c_6}{\Lambda^2}\lambda|H|^6, \tag{1.2}$$

where μ^2 and λ are the conventional parameters employed in the SM potential for the Higgs doublet H.

The changes in the quartic and the triple Higgs couplings, defined in eq. (1.1), are related via [50]:[1]

$$c_3 = c_6, \ d_4 = 6c_6. \tag{1.3}$$

Due to the relation appearing in eq. (1.3), the cross section for triple Higgs boson production is a quartic polynomial in c_6, i.e. it contains terms up to c_6^4. Such terms come from squared matrix elements of diagrams containing two triple Higgs couplings, such as the one shown in figure 1(d).

In figure 3(b) we show the variation of the inclusive leading-order cross sections for ggF hh and hhh with respect to the SM ($c_6 = 0$). The fit as a function of c_6 for the two cases, at 100 TeV, is:

$$\frac{\sigma(c_6)_{hh}}{\sigma(\text{SM})_{hh}} = 0.22 \times c_6^2 - 0.71 \times c_6 + 1.00,$$

$$\frac{\sigma(c_6)_{hhh}}{\sigma(\text{SM})_{hhh}} = 0.03 \times c_6^4 + 0.03 \times c_6^3 + 0.43 \times c_6^2 - 1.31 \times c_6 + 1.00. \tag{1.4}$$

The line $d_4 = 6c_3$ is also shown as a dissection on the $c_3 - d_4$ plane in figure 3(a).

---

[1]Note that, in general, c_3 and d_4 would be multiplied by v^2/Λ^2 in $D = 6$ EFT. We have set $\Lambda = v$ for simplicity here.
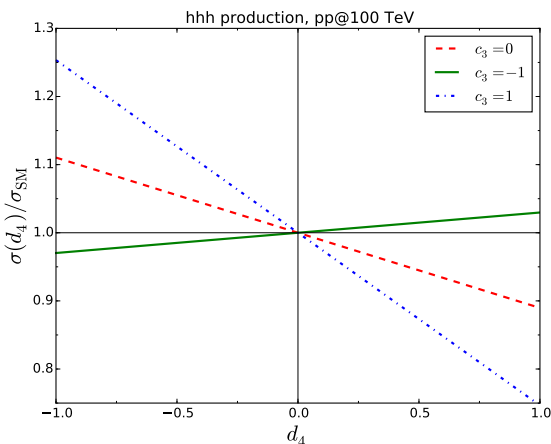
Figure 2. Total cross section ratio normalised to the Standard Model values for gluon-fusion-initiated triple Higgs production at 100 TeV obtained by varying the c_3 and d_4 parameters independently (see eq. (1.1)). The Higgs boson mass was fixed to $m_h = 125$ GeV. The SM cross section at leading order is ~ 2.88 fb. The `NNPDF23_nlo_as_0119` parton density function set was used.
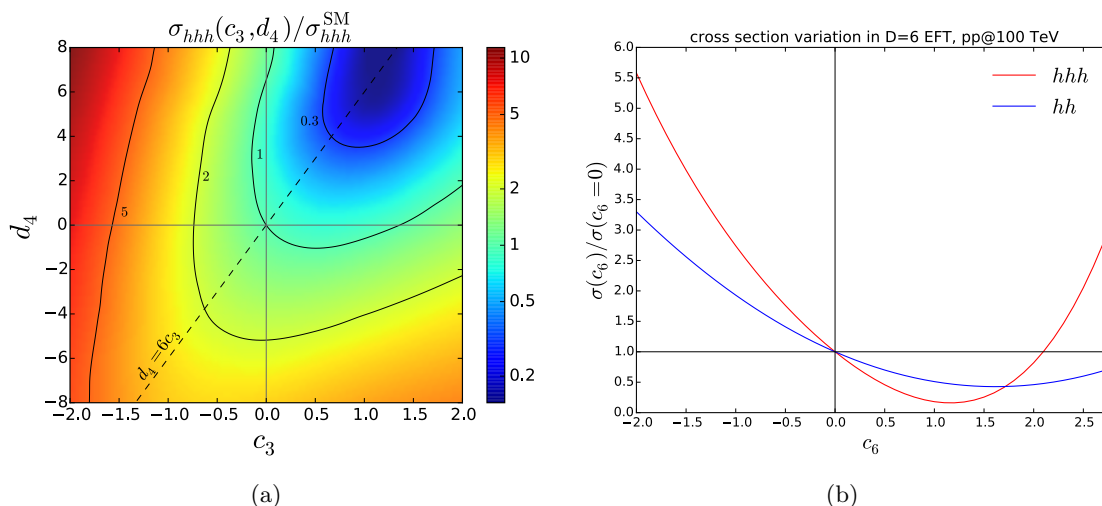

(a)

(b)

Figure 3. Total cross section ratios normalised to the Standard Model values for gluon-fusion-initiated multi-Higgs production at 100 TeV. The Higgs boson mass was fixed to $m_h = 125$ GeV. The SM cross section at leading order is ~ 2.88 fb. On the left-hand panel we show a contour plot of the variation of the cross section ratio with respect to the c_3 and d_4 parameters (see eq. (1.1))). On the right-hand panel one can see the variation with respect to the SM in a theory where the SM is extended with a $\mathcal{O}_6 \sim |H|^6$ operator as in eq. (1.2), for both Higgs boson pair production (hh) and Higgs boson triple production (hhh). For both calculations, the `NNPDF23_nlo_as_0119` parton density function set was used.

2   Triple Higgs production final states

We list the dominant Higgs boson triple production final states, i.e. those that yield $N_{\text{events}} > 10$ with $30\,\text{ab}^{-1}$ of integrated luminosity at a proton collider at 100 TeV centre-of-mass energy, in table 1.

$hhh \to$ final state	BR (%)	σ (ab)	$N_{30\text{ab}^{-1}}$
$(b\bar{b})(b\bar{b})(b\bar{b})$	19.21	1110.338	33310
$(b\bar{b})(b\bar{b})(WW_{1\ell})$	7.204	416.41	12492
$(b\bar{b})(b\bar{b})(\tau\bar{\tau})$	6.312	364.853	10945
$(b\bar{b})(\tau\bar{\tau})(WW_{1\ell})$	1.578	91.22	2736
$(b\bar{b})(b\bar{b})(WW_{2\ell})$	0.976	56.417	1692
$(b\bar{b})(WW_{1\ell})(WW_{1\ell})$	0.901	52.055	1561
$(b\bar{b})(\tau\bar{\tau})(\tau\bar{\tau})$	0.691	39.963	1198
$(b\bar{b})(b\bar{b})(ZZ_{2\ell})$	0.331	19.131	573
$(b\bar{b})(WW_{2\ell})(WW_{1\ell})$	0.244	14.105	423
$(b\bar{b})(b\bar{b})(\gamma\gamma)$	0.228	13.162	394
$(b\bar{b})(\tau\bar{\tau})(WW_{2\ell})$	0.214	12.359	370
$(\tau\bar{\tau})(WW_{1\ell})(WW_{1\ell})$	0.099	5.702	171
$(\tau\bar{\tau})(\tau\bar{\tau})(WW_{1\ell})$	0.086	4.996	149
$(b\bar{b})(ZZ_{2\ell})(WW_{1\ell})$	0.083	4.783	143
$(b\bar{b})(\tau\bar{\tau})(ZZ_{2\ell})$	0.073	4.191	125
$(b\bar{b})(\gamma\gamma)(WW_{1\ell})$	0.057	3.291	98
$(b\bar{b})(\tau\bar{\tau})(\gamma\gamma)$	0.05	2.883	86
$(WW_{1\ell})(WW_{1\ell})(WW_{1\ell})$	0.038	2.169	65
$(\tau\bar{\tau})(WW_{2\ell})(WW_{1\ell})$	0.027	1.545	46
$(\tau\bar{\tau})(\tau\bar{\tau})(\tau\bar{\tau})$	0.025	1.459	43
$(b\bar{b})(WW_{2\ell})(WW_{2\ell})$	0.017	0.956	28
$(WW_{2\ell})(WW_{1\ell})(WW_{1\ell})$	0.015	0.882	26
$(b\bar{b})(b\bar{b})(ZZ_{4\ell})$	0.012	0.69	20
$(\tau\bar{\tau})(\tau\bar{\tau})(WW_{2\ell})$	0.012	0.677	20
$(b\bar{b})(ZZ_{2\ell})(WW_{2\ell})$	0.011	0.648	19
$(\tau\bar{\tau})(ZZ_{2\ell})(WW_{1\ell})$	0.009	0.524	15
$(b\bar{b})(\gamma\gamma)(WW_{2\ell})$	0.008	0.446	13
$(\tau\bar{\tau})(\gamma\gamma)(WW_{1\ell})$	0.006	0.36	10

Table 1. The list of channels with $N_{\text{events}} > 10$ with $30\,\text{ab}^{-1}$ and their branching ratios (BR). The subscript "$_{x\ell}$" denotes the number of leptons x in the final state, originating from the di-bosons. The cross section used for $pp \to hh$ at $100\,\text{TeV}$ is $\sigma_{\text{NLO}} = \sigma_{\text{LO}} \times 2.0 = 5.78\,\text{fb}$, where a K-factor $K = 2.0$ has been applied to obtain an estimate of the NLO cross section. The number of events has been rounded to the nearest integer.

If we apply further requirements to the final states listed in table 1:

- to possess greater than 100 events at 30 ab^{-1} of integrated luminosity,

- and all gauge bosons fully decay to leptons,

then we are left with the following interesting final states: $(b\bar{b})(b\bar{b})(b\bar{b})$, $(b\bar{b})(b\bar{b})(\tau\bar{\tau})$, $(b\bar{b})(b\bar{b})(WW_{2\ell})$, $(b\bar{b})(\tau\bar{\tau})(\tau\bar{\tau})$, $(b\bar{b})(b\bar{b})(\gamma\gamma)$, $(b\bar{b})(\tau\bar{\tau})(WW_{2\ell})$. In particular, the expected combined number of events in the multi-b-jet and multi-τ final states is $\sim$45000 over the

lifetime of the FCC-hh, and will most likely provide valuable information on the triple Higgs boson process. In the present study we focus on the rare but clean final state $(b\bar{b})(b\bar{b})(\gamma\gamma)$.

3 Event generation and detector simulation

3.1 Detector simulation

In the hadron-level analysis that follows, we consider all particles within a pseudorapidity of $|\eta| < 5$ and $p_T > 400\,\mathrm{MeV}$. We reconstruct jets using the anti-k_t algorithm available in the `FastJet` package [82, 83], with a radius parameter of $R = 0.4$. We only consider jets with $p_T > 40\,\mathrm{GeV}$ within $|\eta| < 3.0$ in our analysis. We consider photons within $|\eta| < 3.5$ and $p_T > 40\,\mathrm{GeV}$ and 100% reconstruction efficiency. The jet-to-photon mis-identification probability is taken to be $\mathcal{P}_{j\to\gamma} = 10^{-3}$, flat over all momenta above the p_T cut and over all pseudorapidities.[2] We also consider the mis-tagging of two light jets to bottom-quark-initiated jets with a flat probability of 1% for each mis-tag, corresponding to a flat b-jet identification rate of 80% and demand that they lie within $|\eta| < 3.0$. We demand all photons to be isolated, an isolated photon having $\sum_i p_{T,i}$ less than 15% of its transverse momentum in a cone of $\Delta R = 0.2$ around it. Finally, no detector-smearing effects have been considered.

3.2 Event generation

Events for the hhh signal samples have been generated via the loop-induced module of the `MadGraph 5/aMC@NLO` package [84–88]. The SM loop model present in `MadGraph 5/aMC@NLO` was modified to allow for deformations of the Higgs boson triple and quartic self-couplings away from the SM values. All tree-level and next-to-leading order (i.e. matched via the MC@NLO method [89]) background processes have been generated using `MadGraph 5/aMC@NLO`, apart from the di-Higgs plus jets (hh + jets) background, which was simulated using `HERWIG++` in conjunction with the `OpenLoops` matrix-element generator [32, 90]. The default parton density functions were used in each case: for the signal and tree-level backgrounds (including hh+jets) the `NNPDF23_nlo_as_0119` set was used, whereas for the NLO samples the `NNPDF23_nlo_as_0118_qed` set was employed [91].

Due to the large cross sections and high-multiplicity final states present at a 100 TeV collider, we only generate the tree-level processes to include true photons and true b-quarks at parton level. This implies that light extra jets for these processes will be generated by the parton shower, for which we employ the `HERWIG++` general-purpose event generator [92–95].[3] Inevitably this introduces an uncertainty to the results presented herein, rendering any observables related to these light jets leading-log accurate.[4] We do not expect this, however, to alter the main conclusions of this first, baseline, study. Furthermore, generation-level

---

[2]Note that the HL-LHC expectation has the approximate form $\mathcal{P}_{j\to\gamma} = 0.0093 \times \mathrm{e}^{-0.036 p_{Tj}/\mathrm{GeV}}$ [78]. For a $p_T \sim 40\,\mathrm{GeV}$, this gives approximately $\mathcal{P}_{j\to\gamma} \sim 2 \times 10^{-3}$. Thus, the value employed here is expected to be a reasonable approximation to future detector performance.

[3]Simulation of hadronization and the underlying event were also included. [96]. No simulation of pile-up events was considered.

[4]The hh+jets process is the only exception, with the first jet being leading-order accurate [32].

observable	PS cut
$p_{T,b}$	> 35 GeV, at least one > 70 GeV
$|\eta_b|$	< 3.2
$p_{T,\gamma}$	> 35 GeV, at least one > 70 GeV
$|\eta_\gamma|$	< 3.5
$\Delta R_{\gamma\gamma}$	> 0.2
$m_{\gamma\gamma}$	$\in [90, 160]$ GeV

Table 2. The phase-space (PS) cuts imposed on the background samples $b\bar{b}b\bar{b}$, $b\bar{b}b\bar{b}\gamma$, $b\bar{b}b\bar{b}\gamma\gamma$, $b\bar{b}\gamma\gamma$.

cuts that anticipate the analysis cuts at hadron level are imposed on the b quarks and the photons. In the case of decaying resonances (i.e. h and Z bosons) no cuts are imposed. The phase-space cuts applied on the samples $b\bar{b}b\bar{b}$, $b\bar{b}b\bar{b}\gamma$, $b\bar{b}b\bar{b}\gamma\gamma$, $b\bar{b}\gamma\gamma$ are shown in table 2.

At this point one should stress that even though NLO event generation matched to the parton shower has been largely automated, NLO calculations for the high-multiplicity final states, particularly with many coloured particles and complicated phase space cuts, remain challenging at present. We hence apply a conservatively large flat K-factor of $K = 2.0$ to all the processes calculated at tree level, as well as the hhh and hh+jets loop-induced processes. This is a crucial point that should be addressed in future studies at higher-energy hadron colliders, as such final states will become increasingly common.

The analysis of the signal and backgrounds generated for the final state $(b\bar{b})(b\bar{b})(\gamma\gamma)$ is presented in section 4.2.

4 Analysis

4.1 Differential distributions

We investigate the shape of the differential distributions in Higgs triple production in the Standard Model. Here we keep the Higgs bosons stable and include parton shower effects. We compare the shape of the hhh distributions to those coming from the more familiar case of Higgs boson pair production (hh) at 100 TeV.

Figure 4(a) shows the transverse momentum of any single Higgs boson either in hh or hhh production, $p_{T,h}$. Evidently, the transverse momentum of a Higgs boson in hhh is softer than that of hh, peaking at ~ 100 GeV instead of ~ 150 GeV.

In figure 4(b) we show the the spectrum of the transverse momentum of the Higgs boson "system", p_{T,h^n}, i.e. the triplet of Higgs bosons in hhh, and the two Higgs bosons in hh. One can observe that the p_{T,h^n} is harder in hhh than that of the pair in hh.

We examine the distance between two Higgs bosons, $\Delta R(h, h)$, in hh and hhh production in figure 4(c). In the case of triple production the distance is calculated between any two Higgs bosons. The Higgs bosons in hh are found to be more back-to-back than those in hhh, as expected.
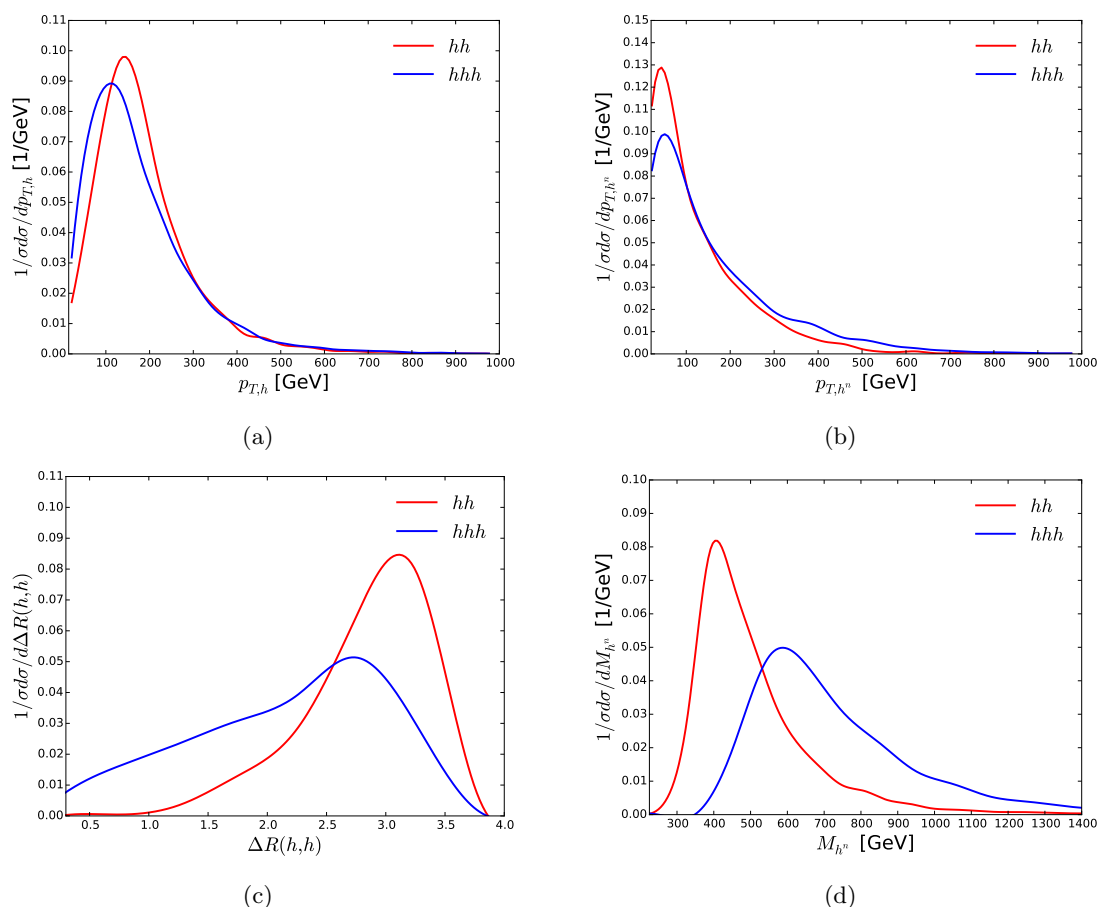
Figure 4. Comparison of differential distributions for Higgs boson pair (hh) and triple production (hhh) in the Standard Model. Parton showering effects are included on top of leading-order matrix elements. Figure (a) shows the transverse momentum of any single Higgs boson, $p_{T,h}$. In (b) we show the the spectrum of the transverse momentum of the Higgs boson "system", p_{T,h^n}, i.e. the triplet of Higgs bosons in hhh, and the two Higgs bosons in hh. In (c) the distance between two Higgs bosons, $\Delta R(h,h)$, is examined and in (d) we show the the invariant mass of all Higgs bosons, M_{h^n}.

Finally, in figure 4(d) we show the the invariant mass of all Higgs bosons in hh or hhh production, M_{h^n}. The invariant mass distribution in hhh peaks just above $M_{h^3} \sim 600\,\mathrm{GeV}$, whereas that in Higgs pair production, just above $M_{h^2} \sim 400\,\mathrm{GeV}$.

4.2 $hhh \to (b\bar{b})(b\bar{b})(\gamma\gamma)$

The $hhh \to (b\bar{b})(b\bar{b})(\gamma\gamma)$ process is expected to be relatively clean and simple to reconstruct.[5] The excellent resolution of the di-photon invariant mass, that has contributed to the Higgs boson discovery at the LHC's Run 1, can be exploited to facilitate background rejection.

---

[5]Note that this final state has been considered in [97], in the context of the two-Higgs doublet model $hH \to hhh$ final state. Here we consider the SM case.

observable	selection cut
$p_{T,b_{\{1,2,3,4\}}}$	$> \{80, 50, 40, 40\}\,\mathrm{GeV}$
$|\eta_b|$	< 3.0
$m_{bb}^{\mathrm{close},1}$	$\in [100, 160]\,\mathrm{GeV}$
$m_{bb}^{\mathrm{close},2}$	$\in [90, 170]\,\mathrm{GeV}$
$\Delta R_{bb}^{\mathrm{close},1}$	$\in [0.2, 1.6]$
$\Delta R_{bb}^{\mathrm{close},2}$	no cut
$p_{T,\gamma_{\{1,2\}}}$	$> \{70, 40\}\,\mathrm{GeV}$
$|\eta_\gamma|$	< 3.5
$\Delta R_{\gamma\gamma}$	$\in [0.2, 4.0]$
$m_{\gamma\gamma}$	$\in [124, 126]\,\mathrm{GeV}$

Table 3. The final selection cuts imposed in the analysis of the $(b\bar{b})(b\bar{b})(\gamma\gamma)$ final state. The observables are defined in the main text.

The present analysis follows a simple path, using the $R = 0.4$ anti-k_t jets as described in section 3. Note, however, that an analysis utilising the jet substructure of boosted Higgses to a bottom-anti-bottom pairs, e.g. as in [98], could assist in signal-background separation. We defer this task to future work.

We ask for four b-jets, or light jets mis-identified as b-jets, within $|\eta| < 3.0$, possessing transverse momenta $p_{T,b_{\{1,2,3,4\}}} > \{80, 50, 40, 40\}\,\mathrm{GeV}$, where the subscripts 1, 2, 3, 4 denote the first, second, third and fourth hardest b-jets respectively. We ask for two photons, or mis-identified jets as photons, within $|\eta| < 3.0$ and $p_{T,\gamma_{\{1,2\}}} > \{70, 40\}\,\mathrm{GeV}$. Due to the fact that, for the majority of b-jets we cannot identify whether they originated from a b-quark or an anti-b-quark, there exists a 3-fold combinatorial ambiguity in combining b-jets into the two Higgs boson candidates. As a simple choice, we take the highest-p_T b-jet and pair it with the closest b-jet in $\Delta R = \sqrt{\Delta\eta^2 + \Delta\phi^2}$, and pair the other two remaining b-jets together.[6] We thus construct the paired b-jet invariant mass, respectively, $m_{bb}^{\mathrm{close},1}$ and $m_{bb}^{\mathrm{close},2}$, for which we demand $m_{bb}^{\mathrm{close},1} \in [100, 160]\,\mathrm{GeV}$ and $m_{bb}^{\mathrm{close},2} \in [90, 170]\,\mathrm{GeV}$. The rather large mass windows are chosen to maintain high signal efficiency given the small initial cross section. Moreover, we construct the distance between the highest-p_T b-jet and the corresponding paired one, and impose $\Delta R_{bb}^{\mathrm{close},1} \in [0.2, 1.6]$.[7] For the photon pair, we simply construct the invariant mass and impose a strong window on the measured Higgs boson mass $m_{\gamma\gamma} \in [124, 126]\,\mathrm{GeV}$.[8] We also restrict the distance between the two photons to $\Delta R_{\gamma\gamma} \in [0.2, 4.0]$. We collect these selection cuts in table 3.

---

[6]We have verified explicitly that an alternative method based on minimization of the squared sum of $(m_{bb} - m_h)$ from each combination yields results that differ by $\mathcal{O}(1\%)$ compared to the simpler ΔR method.

[7]The distance between the other paired b-jets was not found to have significant discriminatory power.

[8]This cut implies that the di-photon resolution should be better than $\sim 1\,\mathrm{GeV}$ at the FCC-hh. The current resolution at the LHC is 1-2 GeV, [99, 100] and thus it is not unreasonable to expect an improvement at the detectors of the future collider.

process	σ_{LO} (fb)	$\sigma_{\mathrm{NLO}} \times \mathrm{BR} \times \mathcal{P}_{\mathrm{tag}}$ (ab)	$\epsilon_{\mathrm{analysis}}$	$N^{\mathrm{cuts}}_{30~\mathrm{ab}^{-1}}$
$hhh \to (b\bar{b})(b\bar{b})(\gamma\gamma)$, SM	2.89	5.4	0.06	9.7
$hhh \to (b\bar{b})(b\bar{b})(\gamma\gamma)$, $c_6 = 1.0$	0.46	0.9	0.04	1.1
$hhh \to (b\bar{b})(b\bar{b})(\gamma\gamma)$, $c_6 = -1.0$	7.94	15.0	0.05	22.5
$b\bar{b}b\bar{b}\gamma\gamma$	1.28	1050	2.6×10^{-4}	8.2
hZZ, (NLO) $(ZZ \to (b\bar{b})(b\bar{b}))$	0.817	0.8	0.002	$\ll 1$
hhZ, (NLO)$(Z \to (b\bar{b}))$	0.754	0.8	0.007	$\ll 1$
hZ, (NLO) $(Z \to (b\bar{b}))$	8.019×10^3	1129	$\mathcal{O}(10^{-5})$	$\ll 1$
$b\bar{b}b\bar{b}\gamma$ + jets	2.948×10^3	2420	$\mathcal{O}(10^{-5})$	$\mathcal{O}(1)$
$b\bar{b}b\bar{b}$ + jets	5.449×10^3	4460	$\mathcal{O}(10^{-6})$	$\ll 1$
$b\bar{b}\gamma\gamma$ + jets	98.7	4.0	$\mathcal{O}(10^{-5})$	$\ll 1$
hh + jets, SM	275.0	592.7	7×10^{-4}	12.4
hh + jets , $c_6 = 1.0$	153.8	331.5	0.001	9.9
hh + jets , $c_6 = -1.0$	518.2	1116.9	4×10^{-4}	13.4

Table 4. The processes considered in the analysis of the $(b\bar{b})(b\bar{b})(\gamma\gamma)$ final state. The parton-level cross section, including the cuts given in the main text is given (if any), the analysis efficiency and the expected number of events at 30 ab^{-1} are given. A flat K-factor of $K = 2.0$ has been applied to all tree-level processes (including hh+jets) as an estimate of the expected increase in cross section from LO to NLO. The hZZ, hhZ and hZ processes have been produced at NLO and hence no K-factor is applied. Even though the hhZ process depends on c_6, we only consider the SM case, as it was found to be negligible after cuts.

We show a summary of the processes considered in the analysis in table 4. The most significant backgrounds in our set-up turn out to be the SM $b\bar{b}b\bar{b}\gamma\gamma$ and those coming from Higgs boson pair production in association with extra jets. Specifically, the latter emulates the signal well, as the di-photon mass window is expected to have similar efficiency to the signal. Moreover, as we have pointed out at the beginning of the section, the Higgs bosons in hh are *harder* on average than than those in hhh, thus passing transverse momentum cuts easily. This background could be tackled in future studies via $h \to b\bar{b}$ tagging using jet substructure techniques that exploit the decay versus the $g \to b\bar{b}$ branching that produces the additional $b\bar{b}$ pair in hh+jets.[9]

4.3 Sensitivity in $D = 6$ EFT

Despite the rather large backgrounds, a signal-to-background ratio of $\mathcal{O}(1)$ can be obtained for the SM case. To summarise the results of the analysis, we present in the first two columns of table 5, respectively, the number of expected hhh events and the total expected number of events, for the SM, as well as for the two simple deformations obtained by including the $D = 6$ operator $\mathcal{O}_6$, with coefficient values $c_6 = \pm 1$. The third column of

---

[9]Note that the additional two b-jets in hh+jets and hZ have been generated by gluon splitting into $b\bar{b}$, performed by the shower Monte Carlo.
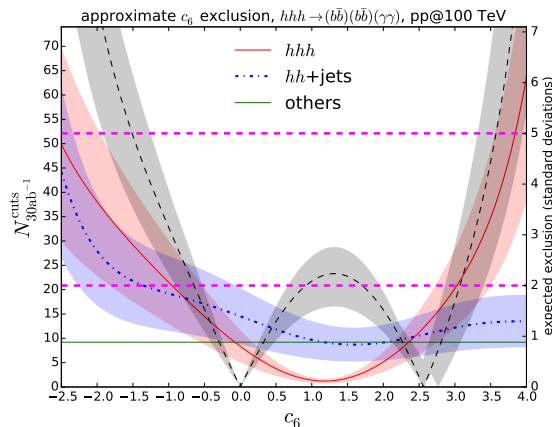
Figure 5. The expected exclusion significance on the c_6 coefficient (right vertical axis), assuming that the theoretical uncertainty on the expected number of hhh and hh+jets events is 40% for each process and uncorrelated between the two. The left vertical axis shows the expected number of events after cuts at 30 ab^{-1}. The horizontal magenta dashed lines show the 2σ and 5σ exclusion points.

table 5 indicates that, if one assumes that the SM is the underlying theory, then $c_6 = \pm 1$ can be excluded at 95% C.L. or better, using $hhh \to (b\bar{b})(b\bar{b})(\gamma\gamma)$ at the 'high-luminosity' phase of the FCC-hh.

Furthermore, we show in figure 5 the expected exclusion region on the c_6 coefficient, as well as the expected number of events after cuts, at 30 ab^{-1}. The theoretical uncertainty on the expected number of events for the hh and the hh+jets processes was taken to be 40% and uncorrelated between the two. The analysis efficiencies for hhh and hh+jets were individually fitted using points in the region $c_6 \in [-3.0, 4.0]$.[10] We assume that there is negligible uncertainty on the 'other' backgrounds, which are taken to consist of the $b\bar{b}b\bar{b}\gamma\gamma$ and $b\bar{b}b\bar{b}\gamma$+jets processes. By examining the central values of the the grey exclusion band, we can see that the regions $c_6 \lesssim -0.7$ and $c_6 \gtrsim 3.0$, as well as the intermediate region $c_6 \in [\sim 1.0, \sim 1.7]$, are expected to be excluded at 95% C.L. (2σ). Moreover, due to the fast-rising hhh cross section, as a function of the c_6 coefficient in this simple model, the 5σ-excluded region lies close to the 2σ outer regions: $c_6 \lesssim -1.4$, $c_6 \gtrsim 3.5$. Note that the analysis can be optimised for each value of c_6 to obtain a higher significance, but in light of the many sources of uncertainties we do not pursue this here. Such optimisation could substantially alter the shape of the hhh and hh+jets curves in figure 5.

4.4 Sensitivity on the $(c_3 - d_4)$-plane

Higgs boson triple production can be used to place constraints on the $(c_3 - d_4)$-plane. This can subsequently be used to impose constraints on arbitrary relations between the triple and quartic coefficients in explicit models. We approximate the hhh signal efficiency over the whole plane by calculating its average value for $c_3 \in [-3.0, 4.0]$, $d_4 = 6c_3$, as obtained in the $D = 6$ EFT example. The analysis is used verbatim, without any modification of

---

[10]The fitting uncertainty is not shown in figure 5.

	hhh	total	$\frac{|N(\mathrm{SM})-N(c_6)|}{\sqrt{N(\mathrm{SM})}}$
SM	9.7	31.3	
$c_6 = 1.0$	1.1	20.2	~ 2.0
$c_6 = -1.0$	22.5	45.1	~ 2.5

Table 5. The number of events for an integrated luminosity of 30 ab^{-1} at 100 TeV, for the Standard Model and the the two simple deformations with $\mathcal{O}_6$, with coefficient values $c_6 = \pm 1$. The first and second columns show, respectively, the number of events for the hhh signal and the total expected number of events for all contributing processes: hhh, hh+jets, $b\bar{b}b\bar{b}\gamma\gamma$ (using 8.2 events) and $b\bar{b}b\bar{b}\gamma$+jets (using 1 event). The third column shows, approximately, the level (in number of standard deviations) at which the two hypotheses $c_6 = \pm 1$ can be excluded given that the standard model is the underlying theory.
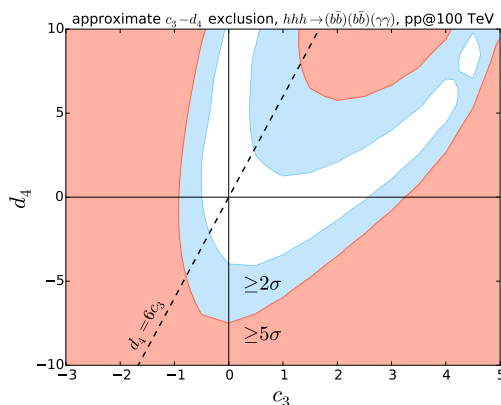

Figure 6. The approximate expected 2σ (blue) and 5σ (red) exclusion regions on the $c_3 - d_4$ plane after 30 ab^{-1} of integrated luminosity, derived assuming a constant signal efficiency, calculated along the $d_4 = 6c_3$ line in $c_3 \in [-3.0, 4.0]$.

cuts along the plane. The standard deviation on the efficiency obtained this way was found to be $\sim 20\%$ along this direction in the given interval. Considering the magnitude of the uncertainties on the signal and background predictions, we consider this to be adequate at present. For the hh+jets background we use the efficiency fit calculated for the $D = 6$ EFT case. We show the projected constraints on the ($c_3 - d_4$)-plane an integrated luminosity of 30 ab^{-1} in figure 6. As a sanity check, we draw the $d_4 = 6c_3$ line and check that the outer 2σ-region: $c_6 \lesssim -2$ and $c_6 \gtrsim 3$ approximately reproduces the $D = 6$ EFT result given the uncertainties. A few interesting observations can be made. Firstly, the whole region $c_3 \lesssim -1$ can be excluded at 5σ irrespective of the value of d_4 using triple Higgs production. Moreover, if c_3 is constrained to lie near $c_3 \sim 0$, then the weakest constraints on d_4 are obtained in all of the plane. On the other hand, if a non-zero value of c_3 is measured, e.g. $c_3 \sim 4$, then the constraint on d_4 can be quite stringent and in a region excluding $d_4 = 0$, i.e. $d_4 \in [\sim 4, \sim 8]$ at 5σ.

5 Discussion and conclusions

Evidently, discovering Standard Model-like triple Higgs boson production will be a challenging task. Our analysis of the $hhh \to (b\bar{b})(b\bar{b})(\gamma\gamma)$ channel has demonstrated that the process merits serious investigation at a future collider running at 100 TeV proton-proton centre-of-mass energy. It is important at this point to emphasise the defining points and caveats that lead this phenomenological analysis to this conclusion:

- The detector of an FCC-hh needs to have excellent photon identification and resolution, so that a di-photon invariant mass window of width 2 GeV around the Higgs boson mass can imposed. As we already mentioned, the current resolution at the LHC is 1-2 GeV, [99, 100]. Moreover, the projections for photon identification efficiency at the high-luminosity LHC are at $\mathcal{O}(80\%)$ [101]. It is not unreasonable to expect an improvement in both of these parameters at the FCC-hh, to a resolution of $\lesssim 1$ GeV or photon identification of $\gtrsim 90\%$.

- Tagging of b-jets should be extremely good, at least in the range of 70-80%, with excellent light jet rejection of $\mathcal{O}(1\%)$ over a wide range of transverse momenta and pseudorapidities. Reducing the tagging probability from 80% to 70% would reduce the final number of events in 'true' 4-b-jet final states by about 40%. We note that the expected performance of the b-tagging algorithms for the LHC Run 2 is already at this ballpark [102].

- Any analysis of triple Higgs production that includes $b\bar{b}$ pairs will also benefit from a very good forward coverage, allowing identification of b-jets up to pseudo-rapidities of $|\eta| \sim 3.0$. Good forward coverage for photons to $|\eta| \sim 3.5$ would also benefit the analysis. For example, the fraction of signal events with two b-jets falling in $|\eta_b| \in [2.5, 3.0]$ is $\sim 15\%$ and the fraction of events with two photons falling in $|\eta_\gamma| \in [2.5, 3.5]$ is $\sim 5\%$. These two are approximately uncorrelated, and thus an LHC-like coverage of $|\eta_b| < 2.5$, $|\eta_\gamma| < 2.5$ would cause a $\sim 20\%$ reduction in signal efficiency compared to the analysis presented in this article.

- Predictions of the triple Higgs boson production cross section, as for the case of double production, posses large theoretical uncertainties at present, due to the unknown higher-order corrections. The best available calculation includes only exact real emission diagrams in combination with 'low-energy theorem' results [15]. A full next-to-leading order calculation will reduce this and allow one to use the process to extract constraints on various models of new physics.

- Crucially, the Monte Carlo event generation of multiple coloured partons (4-6) at next-to-leading order, with complicated phase-space cuts, matched to the parton shower, is essential. Technical improvements in this direction, along with increase in computing power, will allow us to perform predictions with reduced theoretical uncertainties, as well as perform analyses of more hhh final states, such as those mentioned in section 2 (as well as other processes that involve multiple Higgs bosons).

- Due to the aforementioned theoretical and technical limitations, as well as the unknown characteristics of the future collider, we have not attempted to fully quantify the theoretical uncertainties permeating our results. We expect that future improvements in all of these aspects would allow one to obtain a more reliable quantitative result, including a reasonable expectation of uncertainty.

We note here that our event selection is optimised for the assumed detector performance, and if some of these assumptions are changed, the event selection should also be changed to optimise the signal acceptance and background rejection. Moreover in the scenario that the FCC-hh performance is substantially worse than what we have assumed, other channels could come into play, such as $hhh \rightarrow (b\bar{b})(b\bar{b})(\tau^+\tau^-)$ or $hhh \rightarrow (b\bar{b})(\tau^+\tau^-)(\tau^+\tau^-)$.

In conclusion, the study of triple Higgs production should be an important aspect of any future collider programme. It could provide complementary information on the nature of the Higgs boson and its role in electroweak symmetry breaking, as well as extensions of the Higgs boson sector beyond the standard model. This first baseline study resurrects this process and prompts further investigation into how it can be put into use.

Acknowledgments

References

[1] J. Elias-Miro et al., *Higgs mass implications on the stability of the electroweak vacuum*, *Phys. Lett.* **B 709** (2012) 222 [arXiv:1112.3022].

[2] G. Degrassi et al., *Higgs mass and vacuum stability in the Standard Model at NNLO*, *JHEP* **08** (2012) 098 [arXiv:1205.6497] [INSPIRE].

[3] D. Buttazzo et al., *Investigating the near-criticality of the Higgs boson*, *JHEP* **12** (2013) 089 [arXiv:1307.3536] [INSPIRE].

[4] V. Branchina and E. Messina, *Stability, Higgs boson mass and new physics*, *Phys. Rev. Lett.* **111** (2013) 241801 [arXiv:1307.5193] [INSPIRE].

[5] V. Branchina, E. Messina and A. Platania, *Top mass determination, Higgs inflation and vacuum stability*, *JHEP* **09** (2014) 182 [arXiv:1407.4112] [INSPIRE].

[6] F. Bezrukov, J. Rubio and M. Shaposhnikov, *Living beyond the edge: Higgs inflation and vacuum metastability*, *Phys. Rev.* **D 92** (2015) 083512 [arXiv:1412.3811] [INSPIRE].

[7] A.V. Bednyakov, B.A. Kniehl, A.F. Pikelner and O.L. Veretin, *Stability of the electroweak vacuum: gauge independence and advanced precision*, *Phys. Rev. Lett.* **115** (2015) 201802 [arXiv:1507.08833] [INSPIRE].

[8] V. Branchina and E. Messina, *Stability and UV completion of the standard model*, arXiv:1507.08812 [INSPIRE].

[9] E.W.N. Glover and J.J. van der Bij, *Higgs boson pair production via gluon fusion*, *Nucl. Phys.* **B 309** (1988) 282.

[10] S. Dawson, S. Dittmaier and M. Spira, *Neutral Higgs boson pair production at hadron colliders: QCD corrections*, *Phys. Rev.* **D 58** (1998) 115012 [hep-ph/9805244] [INSPIRE].

[11] A. Djouadi, W. Kilian, M. Muhlleitner and P.M. Zerwas, *Production of neutral Higgs boson pairs at LHC*, *Eur. Phys. J.* **C 10** (1999) 45 [hep-ph/9904287] [INSPIRE].

[12] T. Plehn, M. Spira and P.M. Zerwas, *Pair production of neutral Higgs particles in gluon-gluon collisions*, *Nucl. Phys.* **B 479** (1996) 46 [*Erratum ibid.* **B 531** (1998) 655] [hep-ph/9603205] [INSPIRE].

[13] D. de Florian and J. Mazzitelli, *Two-loop virtual corrections to Higgs pair production*, *Phys. Lett.* **B 724** (2013) 306 [arXiv:1305.5206] [INSPIRE].

[14] J. Grigo, J. Hoff, K. Melnikov and M. Steinhauser, *On the Higgs boson pair production at the LHC*, *Nucl. Phys.* **B 875** (2013) 1 [arXiv:1305.7340] [INSPIRE].

[15] F. Maltoni, E. Vryonidou and M. Zaro, *Top-quark mass effects in double and triple Higgs production in gluon-gluon fusion at NLO*, *JHEP* **11** (2014) 079 [arXiv:1408.6542] [INSPIRE].

[16] D. de Florian and J. Mazzitelli, *Higgs pair production at next-to-next-to-leading logarithmic accuracy at the LHC*, *JHEP* **09** (2015) 053 [arXiv:1505.07122] [INSPIRE].

[17] J. Grigo, J. Hoff and M. Steinhauser, *Higgs boson pair production: top quark mass effects at NLO and NNLO*, *Nucl. Phys.* **B 900** (2015) 412 [arXiv:1508.00909] [INSPIRE].

[18] U. Baur, T. Plehn and D.L. Rainwater, *Determining the Higgs boson selfcoupling at hadron colliders*, *Phys. Rev.* **D 67** (2003) 033003 [hep-ph/0211224] [INSPIRE].

[19] U. Baur, T. Plehn and D.L. Rainwater, *Probing the Higgs selfcoupling at hadron colliders using rare decays*, *Phys. Rev.* **D 69** (2004) 053004 [hep-ph/0310056] [INSPIRE].

[20] R. Contino, C. Grojean, M. Moretti, F. Piccinini and R. Rattazzi, *Strong double Higgs production at the LHC*, *JHEP* **05** (2010) 089 [arXiv:1002.1011] [INSPIRE].

[21] R. Grober and M. Muhlleitner, *Composite Higgs boson pair production at the LHC*, *JHEP* **06** (2011) 020 [arXiv:1012.1562] [INSPIRE].

[22] M.J. Dolan, C. Englert and M. Spannowsky, *Higgs self-coupling measurements at the LHC*, *JHEP* **10** (2012) 112 [arXiv:1206.5001] [INSPIRE].

[23] A. Papaefstathiou, L.L. Yang and J. Zurita, *Higgs boson pair production at the LHC in the* $b\bar{b}W^+W^-$ *channel*, *Phys. Rev.* **D 87** (2013) 011301 [arXiv:1209.1489] [INSPIRE].

[24] M.J. Dolan, C. Englert and M. Spannowsky, *New physics in LHC Higgs boson pair production*, *Phys. Rev.* **D 87** (2013) 055002 [arXiv:1210.8166] [INSPIRE].

[25] R. Contino, M. Ghezzi, M. Moretti, G. Panico, F. Piccinini and A. Wulzer, *Anomalous couplings in double Higgs production*, *JHEP* **08** (2012) 154 [arXiv:1205.5444] [INSPIRE].

[26] M. Gillioz, R. Grober, C. Grojean, M. Muhlleitner and E. Salvioni, *Higgs low-energy theorem (and its corrections) in composite models*, *JHEP* **10** (2012) 004 [arXiv:1206.7120] [INSPIRE].

[27] G.D. Kribs and A. Martin, *Enhanced di-Higgs production through light colored scalars*, *Phys. Rev.* **D 86** (2012) 095023 [arXiv:1207.4496] [INSPIRE].

[28] S. Dawson, E. Furlan and I. Lewis, *Unravelling an extended quark sector through multiple Higgs production?*, *Phys. Rev.* **D 87** (2013) 014007 [arXiv:1210.6663] [INSPIRE].

[29] J. Baglio et al., *The measurement of the Higgs self-coupling at the LHC: theoretical status*, *JHEP* **04** (2013) 151 [arXiv:1212.5581] [INSPIRE].

[30] A.J. Barr, M.J. Dolan, C. Englert and M. Spannowsky, *Di-Higgs final states augMT2ed — Selecting hh events at the high luminosity LHC*, *Phys. Lett.* **B 728** (2014) 308 [arXiv:1309.6318] [INSPIRE].

[31] M.J. Dolan, C. Englert, N. Greiner and M. Spannowsky, *Further on up the road: hhjj production at the LHC*, *Phys. Rev. Lett.* **112** (2014) 101802 [arXiv:1310.1084] [INSPIRE].

[32] P. Maierhöfer and A. Papaefstathiou, *Higgs boson pair production merged to one jet*, *JHEP* **03** (2014) 126 [arXiv:1401.0007] [INSPIRE].

[33] J.M. No and M. Ramsey-Musolf, *Probing the Higgs portal at the LHC through resonant di-Higgs production*, *Phys. Rev.* **D 89** (2014) 095031 [arXiv:1310.6035] [INSPIRE].

[34] K. Nishiwaki, S. Niyogi and A. Shivaji, *ttH anomalous coupling in double Higgs production*, *JHEP* **04** (2014) 011 [arXiv:1309.6907] [INSPIRE].

[35] J. Liu, X.-P. Wang and S.-h. Zhu, *Discovering extra Higgs boson via pair production of the SM-like Higgs bosons*, arXiv:1310.3634 [INSPIRE].

[36] T. Enkhbat, *Scalar leptoquarks and Higgs pair production at the LHC*, *JHEP* **01** (2014) 158 [arXiv:1311.4445] [INSPIRE].

[37] Z. Heng, L. Shang, Y. Zhang and J. Zhu, *Pair production of 125 GeV Higgs boson in the SM extension with color-octet scalars at the LHC*, *JHEP* **02** (2014) 083 [arXiv:1312.4260] [INSPIRE].

[38] D.T. Nhung, M. Muhlleitner, J. Streicher and K. Walz, *Higher order corrections to the trilinear Higgs self-couplings in the real NMSSM*, *JHEP* **11** (2013) 181 [arXiv:1306.3926] [INSPIRE].

[39] J. Galloway, M.A. Luty, Y. Tsai and Y. Zhao, *Induced electroweak symmetry breaking and supersymmetric naturalness*, *Phys. Rev.* **D 89** (2014) 075003 [arXiv:1306.6354] [INSPIRE].

[40] U. Ellwanger, *Higgs pair production in the NMSSM at the LHC*, *JHEP* **08** (2013) 077 [arXiv:1306.5541] [INSPIRE].

[41] C. Han, X. Ji, L. Wu, P. Wu and J.M. Yang, *Higgs pair production with SUSY QCD correction: revisited under current experimental constraints*, *JHEP* **04** (2014) 003 [arXiv:1307.3790] [INSPIRE].

[42] M. McCullough, *An indirect model-dependent probe of the Higgs self-coupling*, *Phys. Rev.* **D 90** (2014) 015001 [arXiv:1312.3322] [INSPIRE].

[43] R.S. Gupta, H. Rzehak and J.D. Wells, *How well do we need to measure the Higgs boson mass and self-coupling?*, *Phys. Rev.* **D 88** (2013) 055024 [arXiv:1305.6397] [INSPIRE].

[44] R. Killick, K. Kumar and H.E. Logan, *Learning what the Higgs boson is mixed with*, *Phys. Rev.* **D 88** (2013) 033015 [arXiv:1305.7236] [INSPIRE].

[45] S.Y. Choi, C. Englert and P.M. Zerwas, *Multiple Higgs-portal and gauge-kinetic mixings*, *Eur. Phys. J.* **C 73** (2013) 2643 [arXiv:1308.5784] [INSPIRE].

[46] J. Cao, Z. Heng, L. Shang, P. Wan and J.M. Yang, *Pair production of a 125 GeV Higgs boson in MSSM and NMSSM at the LHC*, *JHEP* **04** (2013) 134 [arXiv:1301.6437] [INSPIRE].

[47] N. Craig, J. Galloway and S. Thomas, *Searching for signs of the second Higgs doublet*, arXiv:1305.2424 [INSPIRE].

[48] F. Goertz, A. Papaefstathiou, L.L. Yang and J. Zurita, *Higgs boson self-coupling measurements using ratios of cross sections*, *JHEP* **06** (2013) 016 [arXiv:1301.3492] [INSPIRE].

[49] F. Goertz, A. Papaefstathiou, L.L. Yang and J. Zurita, *Measuring the Higgs boson self-coupling at the LHC using ratios of cross sections*, arXiv:1309.3805 [INSPIRE].

[50] F. Goertz, A. Papaefstathiou, L.L. Yang and J. Zurita, *Higgs boson pair production in the D = 6 extension of the SM*, *JHEP* **04** (2015) 167 [arXiv:1410.3471] [INSPIRE].

[51] C. Englert, F. Krauss, M. Spannowsky and J. Thompson, *Di-higgs phenomenology in $t\bar{t}hh$: the forgotten channel*, *Phys. Lett.* **B 743** (2015) 93 [arXiv:1409.8074] [INSPIRE].

[52] T. Liu and H. Zhang, *Measuring di-Higgs physics via the $t\bar{t}hh \to t\bar{t}b\bar{b}b\bar{b}$ channel*, arXiv:1410.1855 [INSPIRE].

[53] C.-Y. Chen, S. Dawson and I.M. Lewis, *Top partners and Higgs boson production*, *Phys. Rev.* **D 90** (2014) 035016 [arXiv:1406.3349] [INSPIRE].

[54] R. Frederix et al., *Higgs pair production at the LHC with NLO and parton-shower effects*, *Phys. Lett.* **B 732** (2014) 142 [arXiv:1401.7340] [INSPIRE].

[55] J. Baglio, O. Eberhardt, U. Nierste and M. Wiebusch, *Benchmarks for Higgs pair production and heavy Higgs boson searches in the two-Higgs-doublet model of type II*, *Phys. Rev.* **D 90** (2014) 015008 [arXiv:1403.1264] [INSPIRE].

[56] B. Hespel, D. Lopez-Val and E. Vryonidou, *Higgs pair production via gluon fusion in the two-Higgs-doublet model*, *JHEP* **09** (2014) 124 [arXiv:1407.0281] [INSPIRE].

[57] B. Bhattacherjee and A. Choudhury, *Role of supersymmetric heavy Higgs boson production in the self-coupling measurement of 125 GeV Higgs boson at the LHC*, *Phys. Rev.* **D 91** (2015) 073015 [arXiv:1407.6866] [INSPIRE].

[58] N. Liu, S. Hu, B. Yang and J. Han, *Impact of top-Higgs couplings on Di-Higgs production at future colliders*, *JHEP* **01** (2015) 008 [arXiv:1408.4191] [INSPIRE].

[59] D. Wardrope, E. Jansen, N. Konstantinidis, B. Cooper, R. Falla and N. Norjoharuddeen, *Non-resonant Higgs-pair production in the $b\bar{b}\,b\bar{b}$ final state at the LHC*, [*Eur. Phys. J.* **C 75** (2015) 219](https://...) [[arXiv:1410.2794](https://arxiv.org/abs/1410.2794)] [INSPIRE].

[60] J. Cao, D. Li, L. Shang, P. Wu and Y. Zhang, *Exploring the Higgs sector of a most natural NMSSM and its prediction on Higgs pair production at the LHC*, [*JHEP* **12** (2014) 026](https://...) [[arXiv:1409.8431](https://arxiv.org/abs/1409.8431)] [INSPIRE].

[61] Q. Li, Z. Li, Q.-S. Yan and X. Zhao, *Probe Higgs boson pair production via the $3\ell 2j + \not{E}$ mode*, [*Phys. Rev.* **D 92** (2015) 014015](https://...) [[arXiv:1503.07611](https://arxiv.org/abs/1503.07611)] [INSPIRE].

[62] V. Martín Lozano, J.M. Moreno and C.B. Park, *Resonant Higgs boson pair production in the $hh \to b\bar{b}\,WW \to b\bar{b}\ell^+\nu\ell^-\bar{\nu}$ decay channel*, [*JHEP* **08** (2015) 004](https://...) [[arXiv:1501.03799](https://arxiv.org/abs/1501.03799)] [INSPIRE].

[63] M. van Beekveld et al., *Higgs, di-Higgs and tri-Higgs production via SUSY processes at the LHC with 14 TeV*, [*JHEP* **05** (2015) 044](https://...) [[arXiv:1501.02145](https://arxiv.org/abs/1501.02145)] [INSPIRE].

[64] A. Azatov, R. Contino, G. Panico and M. Son, *Effective field theory analysis of double Higgs boson production via gluon fusion*, [*Phys. Rev.* **D 92** (2015) 035001](https://...) [[arXiv:1502.00539](https://arxiv.org/abs/1502.00539)] [INSPIRE].

[65] N. Liu, Y. Zhang, J. Han and B. Yang, *Enhancing $t\bar{t}hh$ production through CP-violating top-Higgs interaction at the LHC and future colliders*, [*JHEP* **09** (2015) 008](https://...) [[arXiv:1503.08537](https://arxiv.org/abs/1503.08537)] [INSPIRE].

[66] S.M. Etesami and M. Mohammadi Najafabadi, *Double Higgs boson production with a jet substructure analysis to probe extra dimensions*, [*Phys. Rev.* **D 92** (2015) 073013](https://...) [[arXiv:1505.01028](https://arxiv.org/abs/1505.01028)] [INSPIRE].

[67] Z. Kang, P. Ko and J. Li, *New physics opportunities in the boosted di-higgs plus missing-E(T) signature*, [arXiv:1504.04128](https://arxiv.org/abs/1504.04128) [INSPIRE].

[68] S. Dawson, A. Ismail and I. Low, *What's in the loop? The anatomy of double Higgs production*, [*Phys. Rev.* **D 91** (2015) 115008](https://...) [[arXiv:1504.05596](https://arxiv.org/abs/1504.05596)] [INSPIRE].

[69] R. Grober, M. Muhlleitner, M. Spira and J. Streicher, *NLO QCD corrections to Higgs pair production including dimension-6 operators*, [*JHEP* **09** (2015) 092](https://...) [[arXiv:1504.06577](https://arxiv.org/abs/1504.06577)] [INSPIRE].

[70] C.-T. Lu, J. Chang, K. Cheung and J.S. Lee, *An exploratory study of Higgs-boson pair production*, [*JHEP* **08** (2015) 133](https://...) [[arXiv:1505.00957](https://arxiv.org/abs/1505.00957)] [INSPIRE].

[71] H.-J. He, J. Ren and W. Yao, *Probing new physics of cubic Higgs boson interaction via Higgs pair production at hadron colliders*, [*Phys. Rev.* **D 93** (2016) 015003](https://...) [[arXiv:1506.03302](https://arxiv.org/abs/1506.03302)] [INSPIRE].

[72] M.J. Dolan, C. Englert, N. Greiner, K. Nordstrom and M. Spannowsky, *hhjj production at the LHC*, [*Eur. Phys. J.* **C 75** (2015) 387](https://...) [[arXiv:1506.08008](https://arxiv.org/abs/1506.08008)] [INSPIRE].

[73] M. Dall'Osso et al., *Higgs pair production: choosing benchmarks with cluster analysis*, [arXiv:1507.02245](https://arxiv.org/abs/1507.02245) [INSPIRE].

[74] B. Batell, M. McCullough, D. Stolarski and C.B. Verhaaren, *Putting a stop to di-Higgs modifications*, [*JHEP* **09** (2015) 216](https://...) [[arXiv:1508.01208](https://arxiv.org/abs/1508.01208)] [INSPIRE].

[75] S. Dawson and I.M. Lewis, *NLO corrections to double Higgs boson production in the Higgs singlet model*, [*Phys. Rev.* **D 92** (2015) 094023](https://...) [[arXiv:1508.05397](https://arxiv.org/abs/1508.05397)] [INSPIRE].

[76] T. Plehn and M. Rauch, *The quartic Higgs coupling at hadron colliders*, *Phys. Rev.* **D 72** (2005) 053008 [hep-ph/0507321] [INSPIRE].

[77] T. Binoth, S. Karg, N. Kauer and R. Ruckl, *Multi-Higgs boson production in the standard model and beyond*, *Phys. Rev.* **D 74** (2006) 113008 [hep-ph/0608057] [INSPIRE].

[78] A.J. Barr, M.J. Dolan, C. Englert, D.E. Ferreira de Lima and M. Spannowsky, *Higgs self-coupling measurements at a* 100 *TeV Hadron Collider*, *JHEP* **02** (2015) 016 [arXiv:1412.7154] [INSPIRE].

[79] A.V. Kotwal, S. Chekanov and M. Low, *Double Higgs boson production in the* 4τ *channel from resonances in longitudinal vector boson scattering at a* 100 *TeV collider*, *Phys. Rev.* **D 91** (2015) 114018 [arXiv:1504.08042] [INSPIRE].

[80] A. Papaefstathiou, *Discovering Higgs boson pair production through rare final states at a* 100 *TeV collider*, *Phys. Rev.* **D 91** (2015) 113016 [arXiv:1504.04621] [INSPIRE].

[81] D. de Florian and J. Mazzitelli, *Higgs boson pair production at next-to-next-to-leading order in QCD*, *Phys. Rev. Lett.* **111** (2013) 201801 [arXiv:1309.6594] [INSPIRE].

[82] M. Cacciari, G.P. Salam and G. Soyez, *FastJet user manual*, *Eur. Phys. J.* **C 72** (2012) 1896 [arXiv:1111.6097] [INSPIRE].

[83] M. Cacciari and G.P. Salam, *Dispelling the* N^3 *myth for the* k_t *jet-finder*, *Phys. Lett.* **B 641** (2006) 57 [hep-ph/0512210] [INSPIRE].

[84] S. Frixione, F. Stoeckli, P. Torrielli and B.R. Webber, *NLO QCD corrections in HERWIG++ with MC@NLO*, *JHEP* **01** (2011) 053 [arXiv:1010.0568] [INSPIRE].

[85] R. Frederix, S. Frixione, V. Hirschi, F. Maltoni, R. Pittau and P. Torrielli, *Scalar and pseudoscalar Higgs production in association with a top-antitop pair*, *Phys. Lett.* **B 701** (2011) 427 [arXiv:1104.5613] [INSPIRE].

[86] J. Alwall et al., *The automated computation of tree-level and next-to-leading order differential cross sections and their matching to parton shower simulations*, *JHEP* **07** (2014) 079 [arXiv:1405.0301] [INSPIRE].

[87] J. Alwall et al., *Computing decay rates for new physics theories with FeynRules and MadGraph 5_aMC@NLO*, *Comput. Phys. Commun.* **197** (2015) 312 [arXiv:1402.1178] [INSPIRE].

[88] V. Hirschi and O. Mattelaer, *Automated event generation for loop-induced processes*, *JHEP* **10** (2015) 146 [arXiv:1507.00020] [INSPIRE].

[89] S. Frixione and B.R. Webber, *Matching NLO QCD computations and parton shower simulations*, *JHEP* **06** (2002) 029 [hep-ph/0204244] [INSPIRE].

[90] F. Cascioli, P. Maierhofer and S. Pozzorini, *Scattering amplitudes with open loops*, *Phys. Rev. Lett.* **108** (2012) 111601 [arXiv:1111.5206] [INSPIRE].

[91] R.D. Ball et al., *Parton distributions with LHC data*, *Nucl. Phys.* **B 867** (2013) 244 [arXiv:1207.1303] [INSPIRE].

[92] M. Bahr et al., *HERWIG++ physics and manual*, *Eur. Phys. J.* **C 58** (2008) 639 [arXiv:0803.0883] [INSPIRE].

[93] S. Gieseke et al., *HERWIG++ 2.5 release note*, arXiv:1102.1672 [INSPIRE].

[94] K. Arnold et al., *HERWIG++ 2.6 release note*, arXiv:1205.4902 [INSPIRE].

[95] J. Bellm et al., *HERWIG++ 2.7 release note*, arXiv:1310.6877 [INSPIRE].

[96] M. Bahr, S. Gieseke and M.H. Seymour, *Simulation of multiple partonic interactions in HERWIG++*, *JHEP* **07** (2008) 076 [arXiv:0803.3633] [INSPIRE].

[97] V. Barger, L.L. Everett, C.B. Jackson, A.D. Peterson and G. Shaughnessy, *Measuring the two-Higgs doublet model scalar potential at LHC14*, *Phys. Rev.* **D 90** (2014) 095006 [arXiv:1408.2525] [INSPIRE].

[98] D.E. Ferreira de Lima, A. Papaefstathiou and M. Spannowsky, *Standard model Higgs boson pair production in the $(b\bar{b})(b\bar{b})$ final state*, *JHEP* **08** (2014) 030 [arXiv:1404.7139] [INSPIRE].

[99] CMS collaboration, *Search for the standard model Higgs boson decaying into two photons in pp collisions at $\sqrt{s} = 7$ TeV*, *Phys. Lett.* **B 710** (2012) 403 [arXiv:1202.1487] [INSPIRE].

[100] ATLAS collaboration, *Measurement of Higgs boson production in the diphoton decay channel in pp collisions at center-of-mass energies of 7 and 8 TeV with the ATLAS detector*, *Phys. Rev.* **D 90** (2014) 112015 [arXiv:1408.7084] [INSPIRE].

[101] ATLAS collaboration, *Performance assumptions for an upgraded ATLAS detector at a High-Luminosity LHC*, ATL-PHYS-PUB-2013-004 (2013).

[102] ATLAS collaboration, *Expected performance of the ATLAS b-tagging algorithms in Run-2*, ATL-PHYS-PUB-2015-022 (2015).